



Synthesis, Characterization of Polyhedral Oligomeric Silsesquioxane-Metronidazole Conjugate and Determination of Antibacterial, Biocompatible Properties

Idil Karaca Acari*, Ismet Yilmaz, Suleyman Koytepe, Burhan Ates, Sevgi Balcioglu and Turgay Seckin

¹Department of Chemistry, Faculty of Science, Inonu University, 44280, Malatya, Turkey

*Corresponding author: Idil Karaca Acari, Department of Chemistry, Inonu University, Malatya 44280, Turkey, E-Mail: idil.karaca@inonu.edu.tr

Received: August 07, 2018; Accepted: August 20, 2018; Published: September 05, 2018

Abstract

The aim of the present study is to synthesize the antibacterial and biocompatible novel polyhedral oligomeric silsesquioxane-metronidazole (POSS-MTZ) conjugate with condensation reaction from chloro-functional polyhedral oligomeric silsesquioxane and metronidazole. The prepared chloro-functional POSS metronidazole and POSS-metronidazole structures were characterized for their chemical structure; morphology and thermal behaviour by employing fourier transform infrared spectroscopy, ¹H nuclear magnetic resonance spectroscopy, scanning electron microscope/energy dispersive X-ray spectroscopy and thermo gravimetric/differential thermal analysis, differential scanning calorimetric analyzer techniques. In addition, the antibacterial properties of the synthesized POSS-MTZ conjugate were tested with broth micro dilution methods on *E.coli* and *S.aureus* bacteria. The synthesized POSS-MTZ conjugate shows a statistically significant ($p < 0.001$) antibacterial increase in both *E.coli* and *S.aureus* bacteria compared to pure metronidazole (MTZ). Biocompatibility of the POSS-MTZ conjugate was detected in an in vitro cell culture system with an MTT test on L929 mouse skin fibroblast cells. POSS-MTZ conjugates are not cytotoxic. POSS-MTZ conjugate with good biocompatibility and high antibacterial activity can be modified and used for medical and industrial purposes (e.g. wound dressing material, medical surface coating, packaging etc).

Keywords: Polyhedral oligomeric silsesquioxane (POSS); Metronidazole (MTZ); Broth micro dilution;

Biocompatibility; MTT

Introduction

The condensation products of trifunctional silanes are silsesquioxanes. The term “silsesquioxane”, from the Latin prefix “sesqui” means one and a half. The silsesquioxane may contain different structures. For example, it may contain random structures as

well as ladder and cage structures or partial cage structures [1]. Polyhedral oligomeric silsesquioxane (POSS), which belongs to the silsesquioxane family, was first synthesized in 1946. It has a 50 Å cage width and shows rhombohedral crystal structure [2-5]. POSS is a type of three-dimensional, structurally well-defined cage molecule with the general formula $(R_3SiO_1.5)_n$ located between silica (SiO_2) and silicon (R_2SiO) [6]. POSS cage structure is shown in FIG 1.

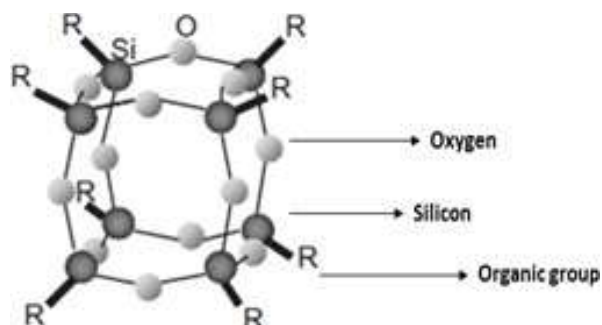


FIG. 1. POSS cage structure.

The inorganic silica-like core is surrounded by organic groups and the cage size is about 1.5 nm [7]. The R group can be hydrogen, alkyl, aryl, arylene or organo-functional alkyl, aryl or aryl derivatives [8]. POSS structures can easily be functionalized by attaching different groups to the eight corners of the cubic structure of POSS [9,10]. The fact that POSS can be functional makes the material very attractive. POSS structures, with properties such as biocompatibility, and chemical and thermal stability, are becoming high performance nanotechnologies for medical, aerospace, mechanical and optoelectronic applications [11,12]. Nitro-containing imidazoles have significant antimicrobial activity. Those such as benzimidazole, secidazole, metronidazole and ornidazole are used clinically [13-15].

The aim of the study was to obtain a new POSS based novel polyhedral oligomeric silsesquioxane-metronidazole (POSS-MTZ) conjugate that exhibits potent antibacterial activity and biocompatibility. Polyhedral oligomeric silsesquioxane-metronidazole (POSS-MTZ) conjugate was synthesized with condensation reaction from chloro-functional polyhedral oligomeric silsesquioxane (POSS-Cl) and metronidazole (MTZ). The prepared POSS-Cl, POSS-MTZ and MTZ structures were characterized for their structure, morphology and thermal behavior by employing fourier transform infrared spectroscopy (FTIR), nuclear magnetic resonance spectroscopy (NMR), scanning electron microscopy with energy dispersive X-ray spectroscopy (SEM/EDX) and the thermal analysis differential thermal analyzer (DTA), thermo gravimetric analyzer (TGA), differential scanning calorimetric analyzer (DSC) techniques. In addition, the antibacterial properties of chloro-functional POSS, metronidazole and the prepared POSS-MTZ conjugate were tested with broth micro dilution methods on *E.coli* and *S.aureus* bacteria's. Biocompatibility of the conjugate was detected in an in vitro cell culture system with the MTT test on L929 mouse skin fibroblast cells.

Materials and Methods

Materials

Most of the chemicals were purchased from Sigma-Aldrich. 3-(4,5- dimethylthiazol-2-yl)-2,5- diphenyltetrazolium bromide (MTT) was purchased from AppliChem. Fetal Bovine Serum (FBS) (from Biowest), Penicillin-Streptomycin (PAN from Biotech), and Dulbecco's Modified Eagle Medium (DMEM) (from Capricorn Scientific). Mouse fibroblast cell line (L929) was subcultured from a stock culture obtained from the Hacettepe University Faculty of Science. Müller Hinton Agar and Müller Hinton Broth (Or-Bak) used in the antibacterial studies of *Escherichia coli* (*E.coli*) ATCC: 25922 and *Staphylococcus aureus* (*S. aureus*) ATCC: 29213 bacteria were obtained from the medical faculty at Inonu University.

Instrumentation

The instruments used in the characterization of the structures are listed here. Infrared spectra were recorded with the ATR technique in the range 4000-650 cm^{-1} on a Perkin Elmer 283 model Fourier transform spectrometer. ^1H NMR spectra were recorded on a Bruker 300 MHz Ultra shield TM prob: 5 mm BBO $^1\text{H}/^{13}\text{C}/^{31}\text{P}/^{15}\text{N}$ instrument and scanned from -0.5 to 11 ppm. Surface analysis and elemental mapping were performed via Leo EV40xVP model scanning electron microscope/energy dispersive X-ray spectroscopy (SEM/EDX). Incident electron beam energies from 3 to 13 keV were used. In all cases, the beam was at normal incidence to the sample surface and the measurement time was 100 s. All the EDX spectra were corrected using the ZAF correction, which takes into account the influence of the matrix material on the obtained spectra. Differential thermal analysis (DTA) and thermogravimetry analysis (TGA) were performed with Shimadzu DTA-50 and TGA-50 thermal analyzers. All the thermal analysis studies were performed at a heating rate of $10^\circ\text{C}/\text{min}$ in an air atmosphere from 20 to 800°C using 10 mg for DTA and TGA. Differential scanning calorimetry (DSC) analysis was performed with a Shimadzu DSC-60. DSC analysis was at $5^\circ\text{C}/\text{min}$ heating rate and under 25 ml/min dynamic nitrogen atmosphere. Analysis was carried out between 300°C and room temperature. The amount of the sample was taken as 10 mg for DSC. The inverted microscope systems (Olympus) were used to observe living cells.

Synthesis of the chloro-functional POSS (POSS-Cl)

The chloro-functional POSS (POSS-Cl) was synthesized from 3-chloropropyltrimethoxysilane by the sol-gel method. 3-chloropropyltrimethoxysilane (45 ml) was added to 100 ml of dry methanol. The concentrated HCl (28 ml) was added to this mixture and stirred for two days at room temperature. PtCl_4 (5 mmol) was added to this solution as the catalyst in an argon atmosphere. The reaction mixture was heated to 50°C and then cooled to room temperature. A white crystalline product was obtained after synthesis [16]. The chloro functional POSS is clearly indicated in FIG. 2.

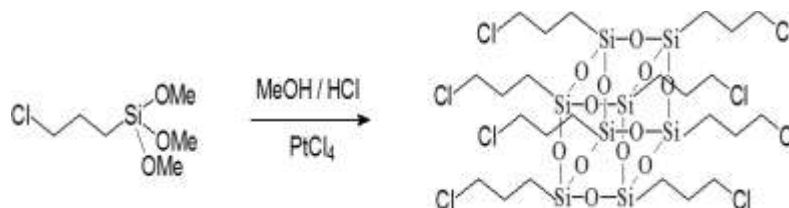


FIG. 2. Synthesis of chloro functional POSS structure.

Synthesis of POSS-MTZ conjugates

The POSS-MTZ conjugate was prepared from octakis (3-chloropropyl)octasilsesquioxane and metronidazole. Metronidazole is a compound containing the imidazole pharmacophore group. At the same time there is an OH group in the construction [17,18]. In synthesis, the molecule is linked to the POSS structure via this OH group. In the experimental phase, the stoichiometric ratio was first determined to be 1/8 for POSS/metronidazole. 5 mmol chloro functional POSS was dissolved in 15 mL DMSO. After the appropriate resolution was obtained, 0.01 g potassium carbonate was added. After stirring for an average of for 4 hours at room temperature, 40 m mol of metronidazole was added and the mixture was refluxed at 60 °C for 30 hours. The desired product was obtained from the resulting white liquid by precipitation. The product was washed and a new POSS-based antibacterial conjugate bearing the imidazole group was obtained. The resulting POSS-MTZ conjugate is clearly indicated in FIG. 3.

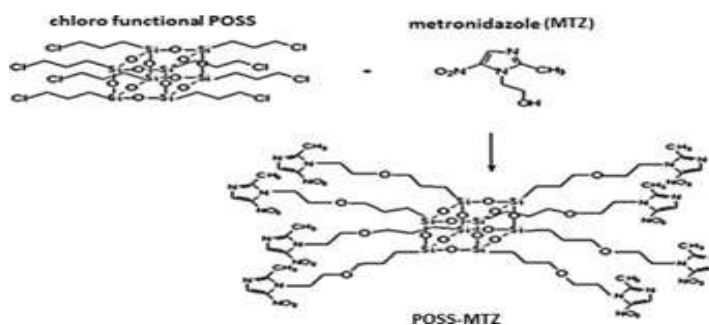


FIG. 3. Synthesis of POSS-MTZ conjugates.

Antibacterial effect of POSS-Cl, MTZ and POSS-MTZ conjugate

The antibacterial activities of the chloro functional POSS, metronidazole and POSS-MTZ conjugate were determined with the widely used broth micro dilution method. According to this method, IC 50 values were determined against *Escherichia coli* (E. coli) ATCC: 25922, and *Staphylococcus aureus* (*S.aureus*) ATCC: 29213. We can sort the experimental stage into four steps. Step 1; 10.000 mg / L stock solutions of chloro functional POSS, MTZ and POSS-MTZ conjugate were prepared. Step 2; the suspension of bacteria to be used in the experiment was prepared. This suspension was performed according to 0.5 McFarland (0.5 McFarland standard is prepared by mixing 0.05 mL of 1.175% BaCl₂.2H₂O with 9.95 mL of 1% H₂SO₄ [19]). Step 3; liquid Müller Hinton broth medium (MHB), sample and bacterial suspension, respectively were applied to the wells in sterile well plates in 96 wells. The last well was chosen as the control. The well plates were left to incubate at 37°C for an average of 18- 24 hours. Step 4; after incubation samples were cultured in solid MHB medium. After the counting process was performed IC50 values were calculated [20-22].

Cell viability POSS-Cl, MTZ, and POSS-MTZ by MTT assay

The quantitative evaluation of cytotoxicity was conducted by MTT assay, which is an assay of metabolism of methyl tetrazolium salt by mitochondrial dehydrogenase of active cells into formazon crystals [23-30]. L929 mouse fibroblast cells in DMEM medium were cultured at 37°C in an incubator containing 5% CO₂. Density of 5000 cells was cultured in 96-well plates and incubated for 24 hours under the same conditions. Samples prepared from stock solutions of 200, 100, 50, 25, and 10 µM concentration were diluted with DMEM medium. 96-well plate attached to the medium of cells was replaced with sample solution. Control wells were replaced with fresh medium. Medium was removed and to the wells were added, respectively, 90 µL DMEM and 10 µL MTT (5mg/mL, in PBS). The same conditions were incubated in the dark for 4 hours and then, after removing the solution from the cells, 100 µL DMSO was added. Absorbance measurements were performed with a micro plate reader at 540 nm. Value of the sample percentage of living cells was detected based on the absorbance results.

Statistical analysis

Statistical analyses were performed with Graphpad Prism 5 software. All data were presented as mean values ± standard deviation.

Results and Discussion

Structural characterization of POSS-Cl, MTZ and POSS-MTZ conjugate by FTIR and 1H NMR

Chloro-functional polyhedral oligomeric silsesquioxane (POSS-Cl), metronidazole (MTZ) and polyhedral oligomeric silsesquioxane-metronidazole (POSS-MTZ) conjugate were characterized by FTIR, ^1H NMR, DTA, TGA, DSC, and SEM/EDX. FIG. 4 shows the FTIR spectra of POSS-Cl, MTZ and POSS-MTZ. Metronidazole is a very small diazole molecule. There is one nitro group and aliphatic methylenes in the structure except for the diazo ring. It also carries one hydroxyl group. The asymmetric NO_2 stretching vibration originating from the nitro groups in the structure is 1505 cm^{-1} and the symmetric NO_2 stretching vibrations occur at 1360 cm^{-1} . We see C-N stretching vibrations at 1442 cm^{-1} on the diazole ring and CH_2 structured C-H peaks with aliphatic character at 925 cm^{-1} . Again, the C-H stretching vibrations of the methylene group of the CH_3 structure in the aliphatic character are at $2846\text{-}2941\text{ cm}^{-1}$ as a binary peak. In the study, pure metronidazole groups are linked via -OH linkage. In the pure metronidazole structure, although the -OH tensile vibration is observed at 3217 cm^{-1} , it is not found in the POSS-metronidazole structure. This finding suggests that metronidazole binds to the POSS structure. When the FTIR spectrum of the POSS-Cl structure is examined, we see a broad Si-O-bond band originating from the POSS structure at $1000\text{-}1100\text{ cm}^{-1}$ in the spectrum and symmetric stretching peaks for the Si-O-Si bond at 928 and 770 cm^{-1} . In these eight functional POSS structures, the very low steric hindrance metronidazole structure was incorporated with a very high yield. In this structure there is the presence of peaks of both Si-O-Si at 1092 cm^{-1} and Si-O stretching peaks at $750\text{-}972\text{ cm}^{-1}$ and the presence of C-N tensile vibrations at 1412 cm^{-1} originating from metronidazole groups. Another indicator of bonding is the C-O-C peak at $1250\text{-}1300\text{ cm}^{-1}$. All these results are evidence that metronidazole is bound to the chloro functional POSS structure.

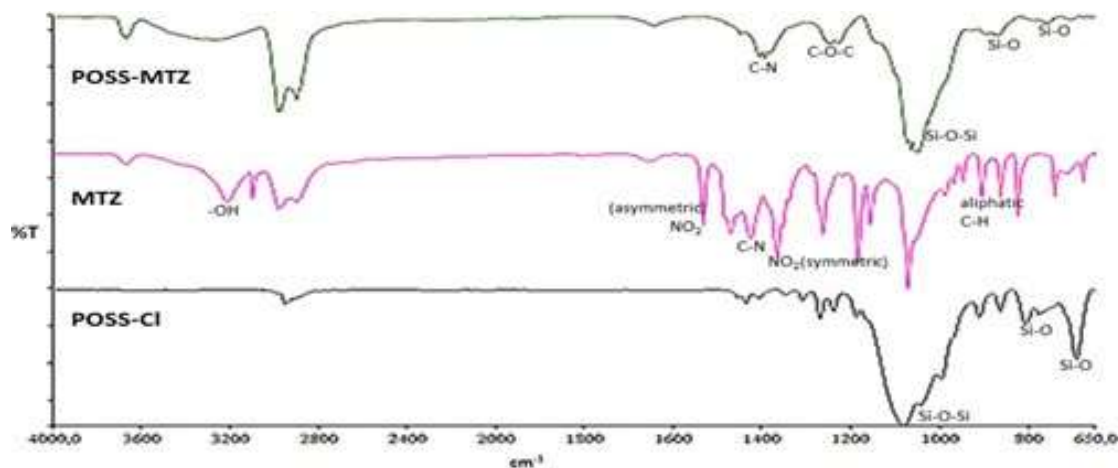


FIG. 4. FTIR spectra of MTZ, POSS-Cl and POSS-MTZ conjugate.

Structural characterization of POSS-Cl, MTZ, and POSS-MTZ conjugate was also made by ^1H NMR (FIG. 5-7). For POSS-Cl ^1H NMR (DMSO, d_6), 2.70 ppm proton of $\text{Si-CH}_2\text{CH}_2\text{Cl}$, 1.81 ppm proton of SiCH_2CH_2 and at 0.91 ppm peaks of SiCH_2 protons are visible. 8.03 ppm, the C-H proton attached to the aromatic ring found in the pure metronidazole structure, is

visible as is 5.05 ppm proton of the N-CH₂ group. At 4.49 ppm, CH₂ protons related to the OH group, which is a more electronegative group, are seen and the CH₂ groups attached to the aromatic ring structure are found at 3.71 ppm. The CH₂-CH₂ structure with aliphatic character is clearly visible at 3.38 ppm.

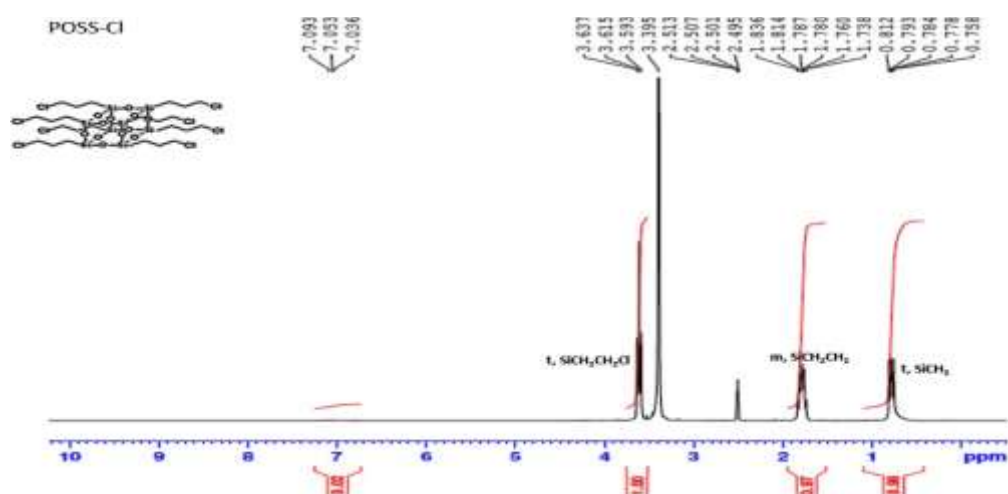


FIG. 5. ¹H NMR spectra of POSS-Cl.

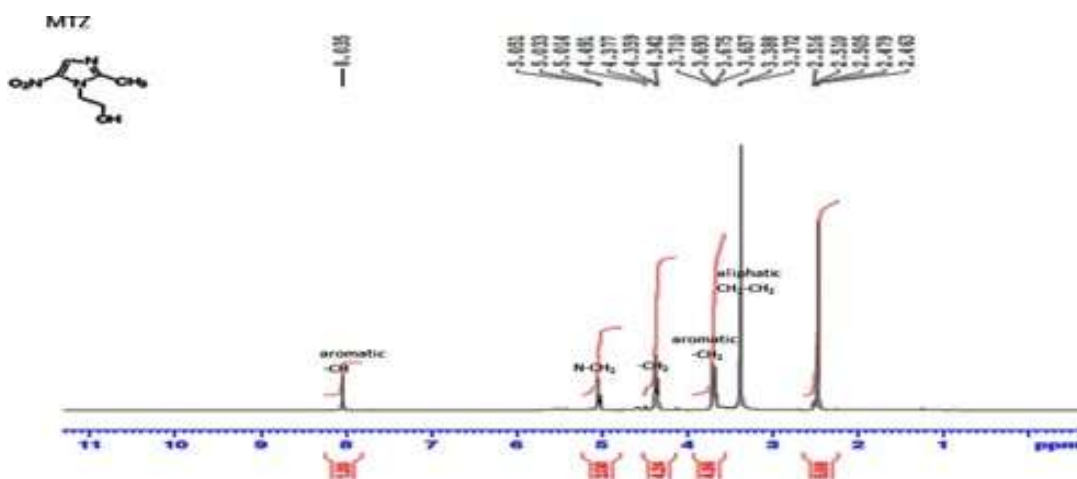


FIG. 6. ¹H NMR spectra of MTZ.

When we look at the POSS-MTZ structure, we see the aliphatic CH₂ groups at 2.55 ppm proton of Si-CH₂ and 3.69 ppm proton of Si-CH₂CH₂, and at 4.36 ppm proton of aliphatic CH₂ and 5.03 ppm proton of N-CH₂. And finally at 8.01 ppm we

see the C-H peaks of aromatic structures. The appearance of aromatic peaks in the POSS structure with aliphatic character proves that the metronidazole structure is bound.

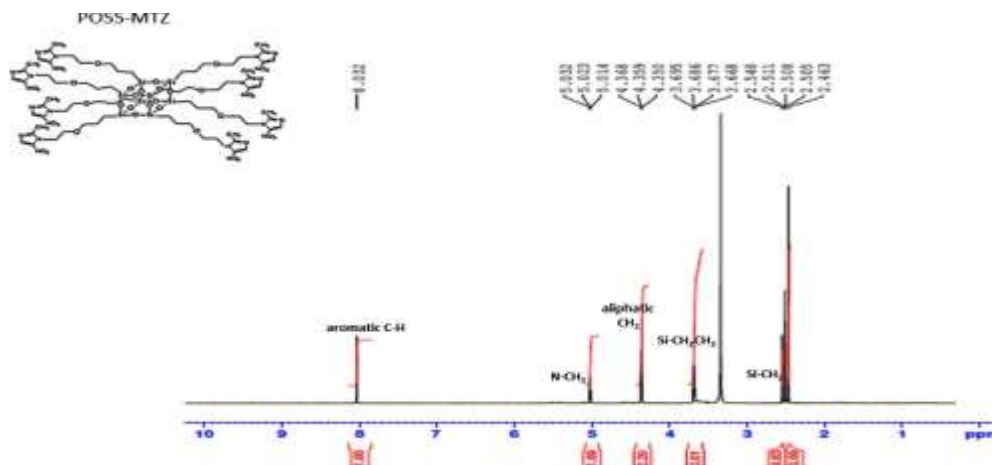


FIG. 7. ^1H NMR spectra of POSS-MTZ conjugate.

Thermal analysis of POSS-Cl, MTZ and POSS-MTZ conjugate

Thermal analysis results were obtained with TGA, DTA and DSC techniques. TGA, DTA and DSC results are given respectively in FIG. 8-10. In FIG. 8, when TGA is examined, the total decomposition temperature of the chloro POSS structure starts at 325°C. Mass loss of 50% occurred. The degradation temperature of the metronidazole molecule is observed at 170°C. Degradation occurred in a very narrow temperature range and ended at 225°C. In the case of the POSS-MTZ structure, loss of mass of metronidazole groups attached to the POSS structure was observed in a similar temperature range. In FIG. 9, the degradation of the chloropropyl side groups of the corresponding molecules was observed at 350-565°C in the DTA thermo grams. In the thermo gram of the metronidazole molecule, a small deformation was observed between 100 and 250°C followed by a sharp thermal deformation. In the case of the POSS-MTZ structure, the basic disruption starts at around 221°C. Structural disruption is a fundamental band appearance. It has a wide band appearance between 235-735°C. DSC thermo grams of POSS-Cl, MTZ, and POSS-MTZ are given in FIG. 10. In these thermo grams, the metronidazole structure seems to be degraded by a very sharp peak at 250-305°C. However, when connected to the POSS structure, the disruption peak rises to 320°C. This demonstrates the contribution of the POSS molecule to the antibiotic structure. Again, in these thermo grams, the melting point of the metronidazole group is observed at 150°C. The melting point of the POSS-MTZ structure is 120°C. A significant change in this value indicates a binding to the structure.

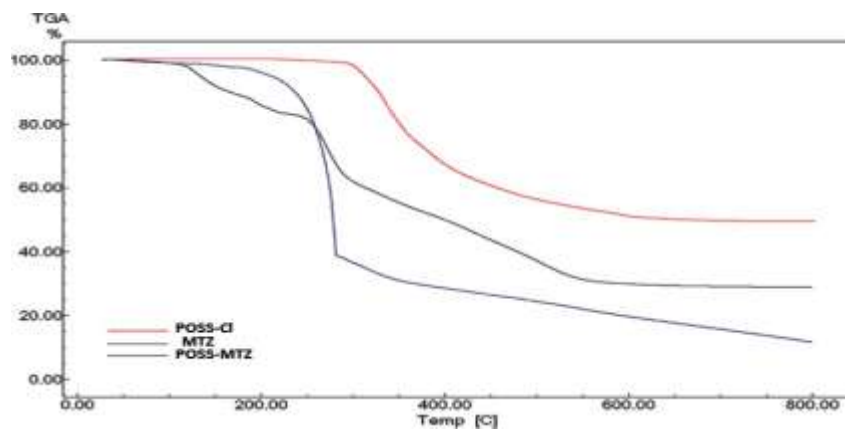


FIG. 8. TGA thermograms of POSS-Cl, MTZ and POSS-MTZ conjugate.

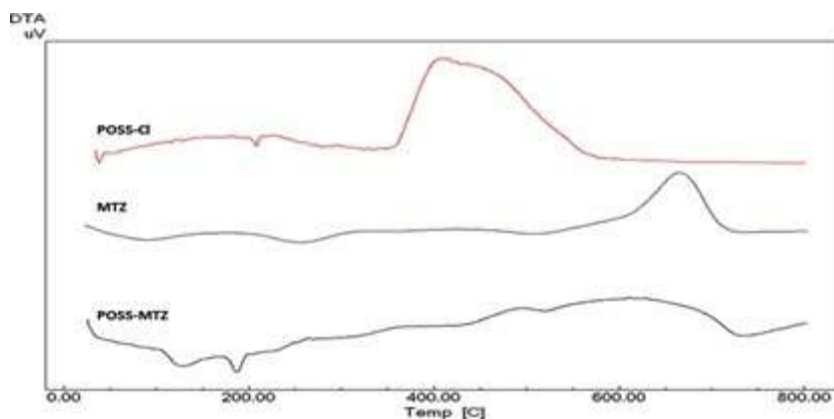


FIG. 9. DTA thermograms of POSS-Cl, MTZ and POSS-MTZ conjugate.

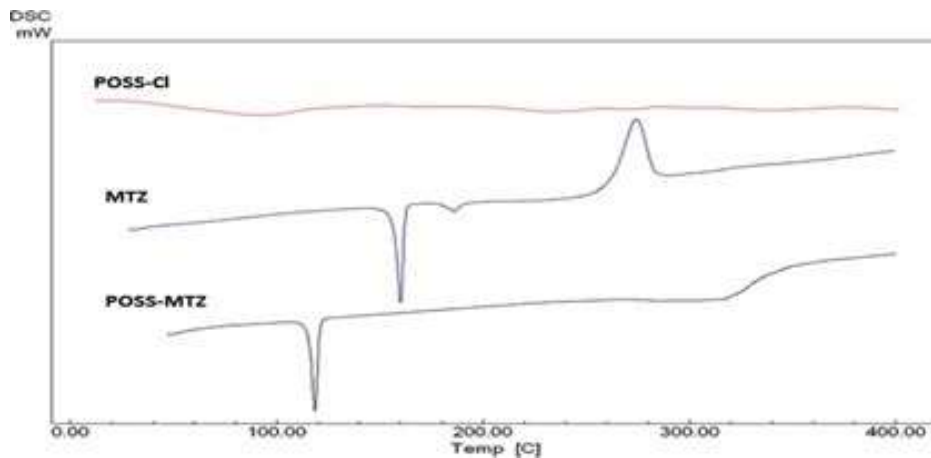


FIG. 10. DSC thermo grams of POSS-Cl, MTZ and POSS-MTZ conjugate.

Surface analysis of POSS-Cl, MTZ and POSS-MTZ conjugate

In FIG. 11, SEM images of POSS-Cl, MTZ and POSS-MTZ structures are given. When the POSS-Cl structure is examined in FIG. 11a and 11b, a fractal and homogeneous surface appearance is seen. At high magnification this fractal structure is more visible. FIG 11c and 11d show SEM images of the metronidazole structure. This SEM image shows that the metronidazole structure has a fractal surface like the POSS structure. Unlike POSS, however, it is a smaller piece. The POSS-MTZ structure exhibits a very different surface appearance than the starting materials. It is more crystalline and planar. The entire structure is seen as homogeneous. Cubic crystal formations exist. This change proves to us that a new structure has been established. The EDX spectra of POSS-Cl, MTZ and POSS-MTZ conjugate can be seen in FIG. 12. We clearly see the C, O, Si and Cl peaks of the POSS-Cl structure in FIG. 12A. We can see C (0.277 keV), O (0.523 keV), Si (1.743 keV) and Cl ($K\alpha$ 0.183 keV and $K\beta$ 2.622 keV) peaks in spectral maps. FIG. 12b shows an EDX image of the MTZ structure. In this spectrum, C (0,277 ke V), N (0,392 keV), and O (0,523 keV) peaks are seen. Furthermore, in order to provide solubility in the preparation of the conjugate, the elements Ca and P have been observed incorporated into the structure. When we look at the POSS-MTZ conjugate in FIG. 12c we see elements coming from both POSS and MTZ structures. Observation of a very low amount of chlorine is an indication of the existence of the desired POSS-MTZ product with a high yield.

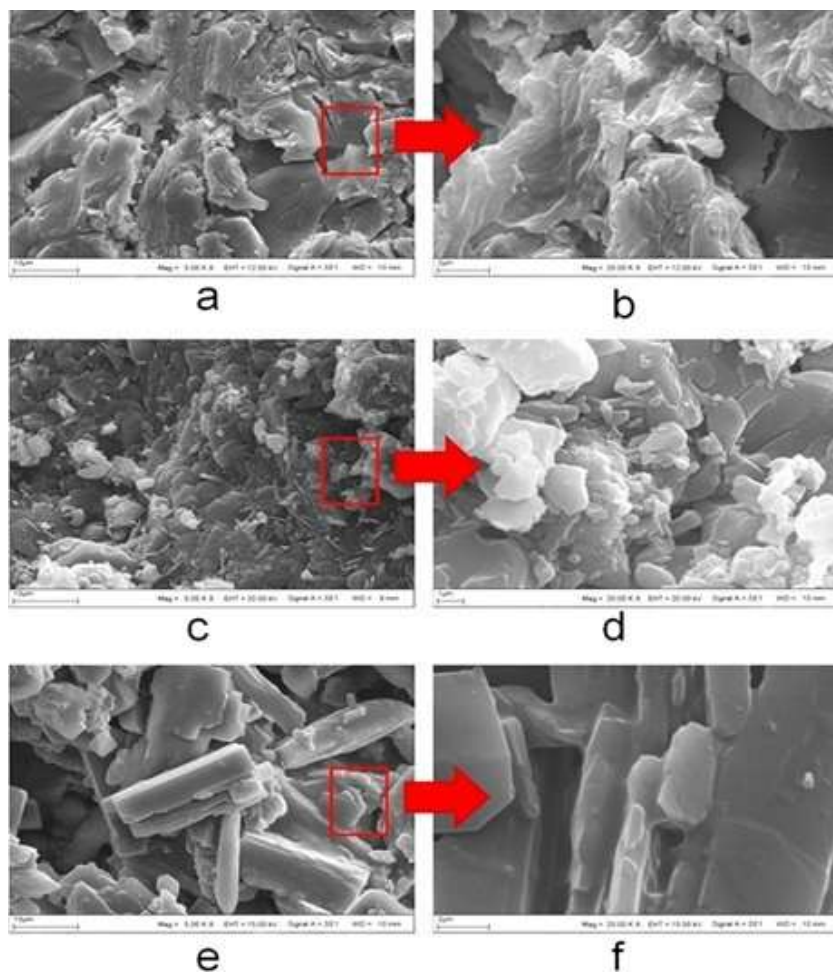


FIG. 11. (a,b) SEM images of POSS-Cl. (c,d) SEM images of MTZ. (e,f) SEM images of POSS-MTZ conjugate.

Antibacterial activity results of POSS-Cl, MTZ, and POSS-MTZ conjugate Antibacterial activity was tested against *E.coli* and *S.aureus* bacteria. It was determined according to the broth micro dilution method. Antibacterial activity for control and POSS-Cl were not determined for *E.coli* and *S.aureus* bacteria. IC50 values of the MTZ and POSS-MTZ conjugates showing antibacterial activity are given in FIG. 13. IC50 value of MTZ was found to be 1933.33 ± 115.47 mg/L for *E.coli* and 1416.67 ± 144.33 mg/L for *S.aureus*. However, the IC50 value of POSS-MTZ conjugate was measured at 304.17 ± 7.22 and 260 ± 17.32 mg/L for *E.coli* and *S.aureus*, respectively. When we look at the IC₅₀ values, we see that a new POSS-based antibacterial conjugate is obtained that is more effective than an average six times pure MTZ.

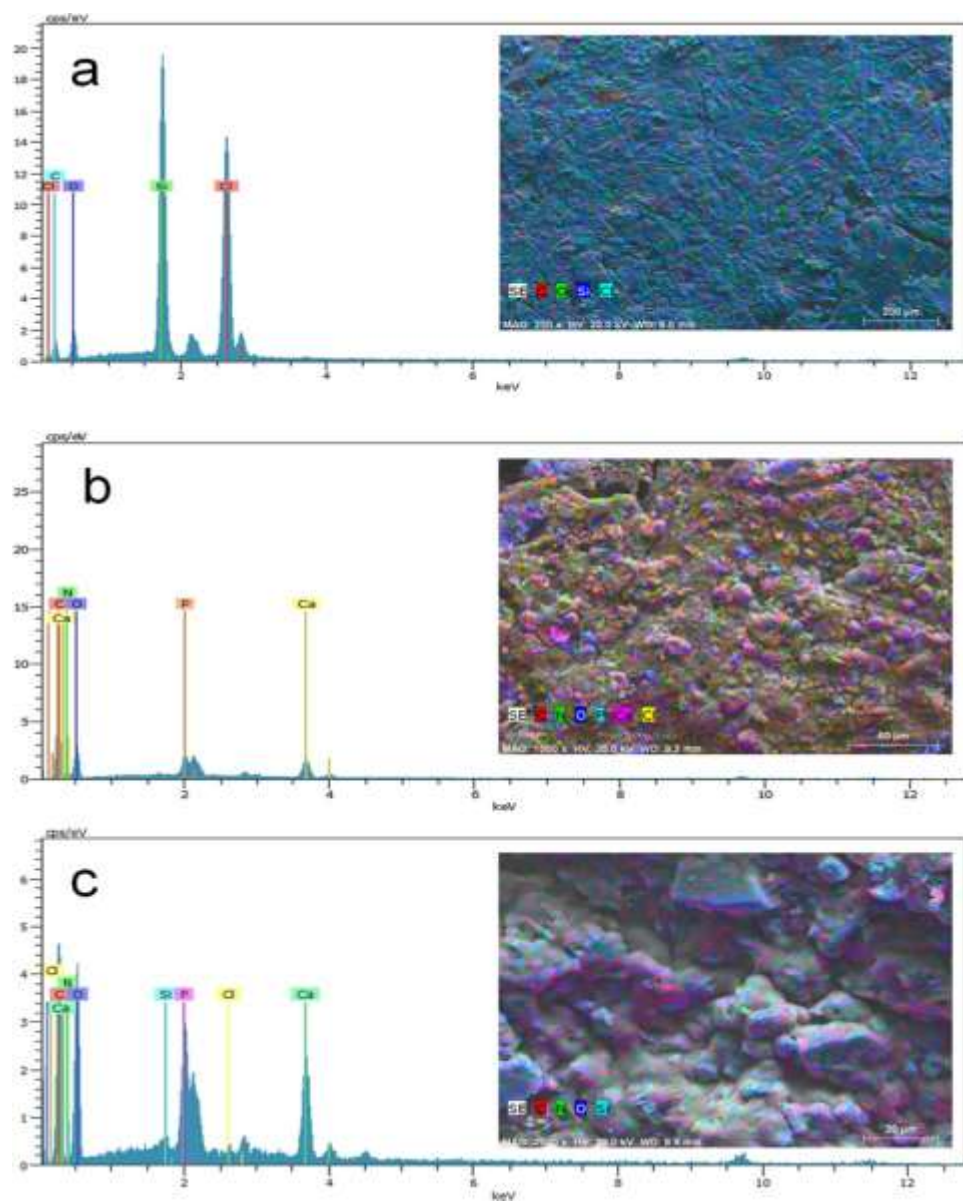


FIG. 12. (a) EDX elemental mapping images for POSS-Cl. (b) EDX elemental mapping images for MTZ. (c) EDX elemental mapping images for POSS-MTZ conjugate.

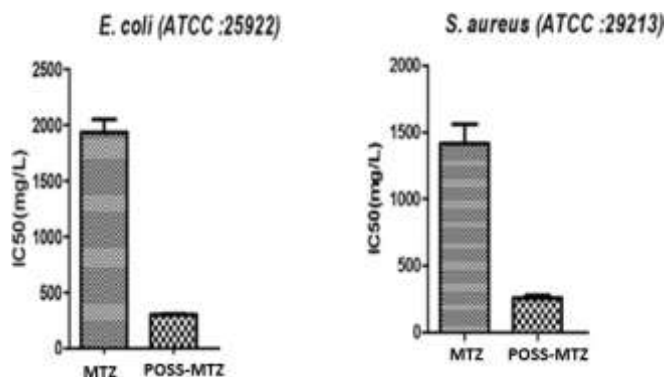


FIG. 13. IC₅₀ values for MTZ and POSS-MTZ conjugate.

Cell culture cytotoxicity results for POSS-Cl, MTZ, and POSS-MTZ conjugate Cytotoxicity test results were successfully performed on L929 mouse skin fibroblast cells. Cytotoxicity test results and cell images are shown in FIG. 14. According to ISO-10993-5, the inhibition of cell viability by more than 30% is considered as a cytotoxic effect for biomaterials. POSS-MTZ conjugate exhibited high cell viability (>90%) in range from 25 to 200 μ M. These results were also evaluated as Grade 1 according to ISO standards. It has been experimentally proven that the POSS-Cl, MTZ and POSS-MTZ conjugates are not cytotoxic in L929 fibroblast cells.

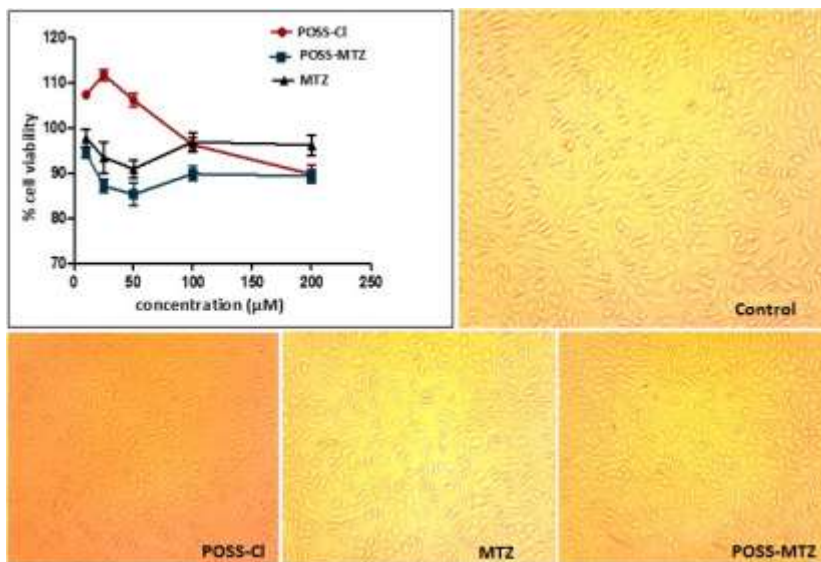


FIG. 14. Cell viability results and images for Control, POSS-Cl, MTZ and POSS-MTZ conjugate.

Conclusion

It has been proven that the POSS-MTZ conjugate based on POSS was successfully synthesized using FTIR, NMR, SEM/EDX and TGA, DTA, DSC techniques. The newly synthesized POSS-MTZ conjugate showed a statistically significant ($p < 0.001$) antibacterial increase in both *E.coli* and *S.aureus* bacteria's compared to pure MTZ. IC50 value of MTZ was found to be 1933.33 ± 115.47 mg/L for *E.coli* and 1416.67 ± 144.33 mg/L for *S.aureus*. However, IC50 value of POSS-MTZ conjugate was measured at 304.17 ± 7.22 and 260 ± 17.32 mg/L for *E.coli* and *S.aureus*, respectively. When we look at the IC50 values, we see that a new POSS-based antibacterial POSS-MTZ conjugate is obtained that is more effective than an average six times pure MTZ. In addition, the POSS-MTZ conjugate showed high cell viability, (almost $\square 100\%$) in the in vitro cell cytotoxicity test. The new POSS-MTZ conjugate with high antibacterial activity and good biocompatibility can be modified and used for medical and industrial purposes (e.g. wound dressing material, medical surface coating, packaging etc.)

Acknowledgements

This work was supported by Inonu University's scientific research projects unit (BAP) with code 2013/157.

REFERENCES

1. K. Kanamori, K. Nakanishi; Chem.Soc.Rev, 40, 754-770 (2011)
2. K. Pielichowski, J. Njuguna, B. Janouski, J. Pielichawski; Adv Polym Science. 201, 225-296 (2006).
3. R.H. Baney, M. Hoh, A. Sakakibara, T. Suzuki; Chem. Rev., 95, 1409-1430 (1995).
4. V. Belot, R. Corriu, D. Leclerg, A. Vioux; Chem. Mater. 3, 127-131(1991).
5. T. Seçkin, S. Köytepe, H.İ. Adıgüzel; Mater Chem Phys. 112, 1040-1046 (2008).
6. D.B. Cordes, P.D. Lickiss, F. Rataboul; Chem. Rev. 110, 2081-2173 (2010).
7. H. Fan, J. He, R. Yang; Appl. Polym. Sci. 127, 463-470 (2013).
8. K. Kanamori, K. Nakanishi; Chem.Soc.Rev. 40, 754-770 (2011).
9. G.Z. Li, H.N. Wang, C.U. Pittman; J Inorg Organomet Polym. 11,123-154 (2001).
10. G.Z. Li, T. Yamamoto, K. Nozaki, M. Hikosaka; Polymer. 42, 8435-8441 (2009).
11. J. Wu, P.T Mather; J of Macromolecular Science. 49, 25-63 (2009).
12. G. Punshon, D.S. Vara, K.M. Sales, A.G. Kidane, H.J. Salacinski, A.M. Seifalian; Biomaterials. 26, 6271-6279 (2005).
13. S. Khabnadideh, Z. Rezaei, N.A. Khalafi, M.H. Motazedian; J. Pharm. Sci. 15, 17-20 (2007).
14. C.F. Redigueri, V. Porta, D.S. G. Nunes, T.M. Nunes, H.E. Junginger, S. Kopp, K.K. Midha,
15. V.P. Shah, S. Stavchansky, J.B. Dressman, D.M. Barends; J Pharm Sci. 100, 1618-1627 (2011).

16. E.D. Ralph, D.A. Clarke; *Antimicrob Agents Chemother.* 14, 377-383 (1978).
17. M.H. Demirel, S. Köytepe, A. Gültek, T. Seçkin; *J Polym Res.* 21, 345. (2014).
18. L. Zhang, J-J. Chang, S-L, Zhang, G.L.V. Damu, R-X. Geng, C-H. Zhou; *Bioorg. Med. Chem.* 21, 4158-4169 (2013).
19. V. Porta, D.S.G. Nunes, T.M. Nunes, H.E. Junginger, S. Kopp, K.K. Midha, V.P. Shah, S. Stavchansky, J.B. Dressman, D.M. Barends, C.F. Rediguieri; *J. Pharm. Sci.*100, 1618-27 (2011).
20. M. Balouiri, M. Sadiki, S.K. Ibsouda; *J. Pharm. Anal.* 6, 71-79 (2016).
21. P. Lubber, E. Bartelt, E. Genschow, J. Wagner, H. J. Hahn; *Clin. Microbiol.* 41, 1062-1068 (2003).
22. M. Kidwai, S. Saxena, M.K.R. Khan, S.S. Thukral; *Bioorg.Med. Chem. Lett.* 4295-4298 (2005).
23. P. Polcyn, M. Jurczak, A. Rajnisz, J. Solecka, Z. Urbanczyk-Lipkourska; *Molecules.* 6, 71- 79 (2016).
24. S.H. Bae, J-H. Che, J-M. Seo, J. Jeong, E.T. Kim, S.W. Lee, K. Koo, G.J. Suaning, N.H. Lovell, D.D. Cho, S.J. Kim, H. Chung; *Invest Ophthalmol Vis Sci.* 53, 2653-7 (2012).
25. M. Ferrari, M.C. Fornasiero, A.M. Isetta; *J. Immunol. Methods.* 131, 165-172 (1990).
26. T. Selvarani, B.K. Prabhu, K. Thenmozhi; *Int.J. Med.* 3, 169-177 (2013).
27. F. Chen, T. Wu, X. Cheng; *Gerodontology.*31, 4-10 (2014).
28. S. Balcioglu, H. Parlakpınar, N. Vardi, E.B. Denkbaz, M.G. Karaaslan, S. Gulgen, E. Taslidere, S. Koytepe, B. Ates; *Appl. Mater. Interfaces.* 8, 4456-4466 (2016).
29. H.Y. Jo, Y. Kim, H.W. Park, H.E. Moon, S. Bae, J.W. Kim, D.G. Kim, S.H. Paek; *Exp. Neurobiol.* 24, 235-245 (2015).
30. B. Mitrovic, L.J. Ignarro, S. Montestruque, A. Small, J.E. Merrill, *Neuroscience.* 61, 575-585 (1994).